Received: 19 February 2019 | Revised: 13 June 2019 | Accepted: 22 July 2019

DOI: 10.1002/asl.937

RESEARCH ARTICLE

Atmospheric Science Letters RMetS

Suppressed eddy driving during southward excursions of the North Atlantic jet on synoptic to seasonal time scales

Erica Madonna[1,2] | **Camille Li**[1,2] | **Justin J. Wettstein**[3,2,1]

[1]Geophysical Institute, University of Bergen, Bergen, Norway

[2]Bjerknes Centre for Climate Research, Bergen, Norway

[3]College of Earth, Ocean, and Atmospheric Sciences, Oregon State University, Corvallis, Oregon

Correspondence
Erica Madonna, Geophysical Institute, University of Bergen, Postbox 7803, N-5020 Bergen, Norway.
Email: erica.madonna@uib.no

Funding information
Research Council of Norway, Grant Numbers: 231716 and 255027

Abstract

Jet streams shape midlatitude weather and climate. The North Atlantic jet is mainly eddy-driven, with frequent north–south excursions on synoptic time scales arising from eddy forcings and feedbacks. There are, however, special periods during which the underlying dynamics appear to change—for example, winter 2009/2010, when the jet was persistently southward-shifted, extremely zonal, and more thermally driven. This study shows evidence that the southern jet configuration exhibits altered dynamical behavior involving a shift in the balance of thermal and eddy-driving processes, independent of timescale. Specifically, southern jets exhibit weaker eddy feedbacks and are associated with enhanced heating in the tropical Pacific. During winter 2009/2010, a remarkably frequent (66 days out of the 90-day winter season) and persistent southern jet shaped the unusual seasonal signature. These results bridge the synoptic and climate perspectives of jet variability, with potential to help understand and reduce biases in regional climate variability as simulated by models.

KEYWORDS

climate variability, eddy-mean flow interactions, jet stream, North Atlantic

1 | INTRODUCTION

Jet streams are fundamental components of the atmospheric circulation. Two mechanisms are responsible for their existence: (1) eddy driving, whereby atmospheric waves converge westerly momentum to form a deep barotropic jet that balances mechanical dissipation at the surface (Held, 1975; Rhines, 1975; Panetta, 1993), and (2) thermal driving, whereby angular momentum conservation in the Hadley circulation forms a subtropical jet confined to the upper troposphere (Schneider, 1977; Held and Hou, 1980). Idealized modeling simulations suggest that when thermal driving (tropical heating) is weak, eddies grow in the baroclinic zone situated poleward of the subtropical jet and produce a distinct eddy-driven jet (Son and Lee, 2005). When tropical heating is strong, a single, merged jet develops (Lee and Kim, 2003; Son and Lee, 2005). In the North Atlantic sector two well-separated jets are observed during winter—the primarily eddy-driven North Atlantic jet at about 46°N and the primarily subtropical (thermally driven) African jet at about 18°N (Figure 1, blue contours). In contrast, the North Pacific is characterized by a merged jet located at about 35°N and exhibiting the influence of both driving processes (Eichelberger and Hartmann, 2007; Li and Wettstein, 2012).

Jet streams exhibit large variability over a range of time scales. The dominant mode of interannual variability depends on the dominant driving process: a meridional shifting for eddy-driven jets, and a pulsing or extension/retraction for thermally-driven or merged jets (Eichelberger and Hartmann, 2007; Athanasiadis *et al.*,

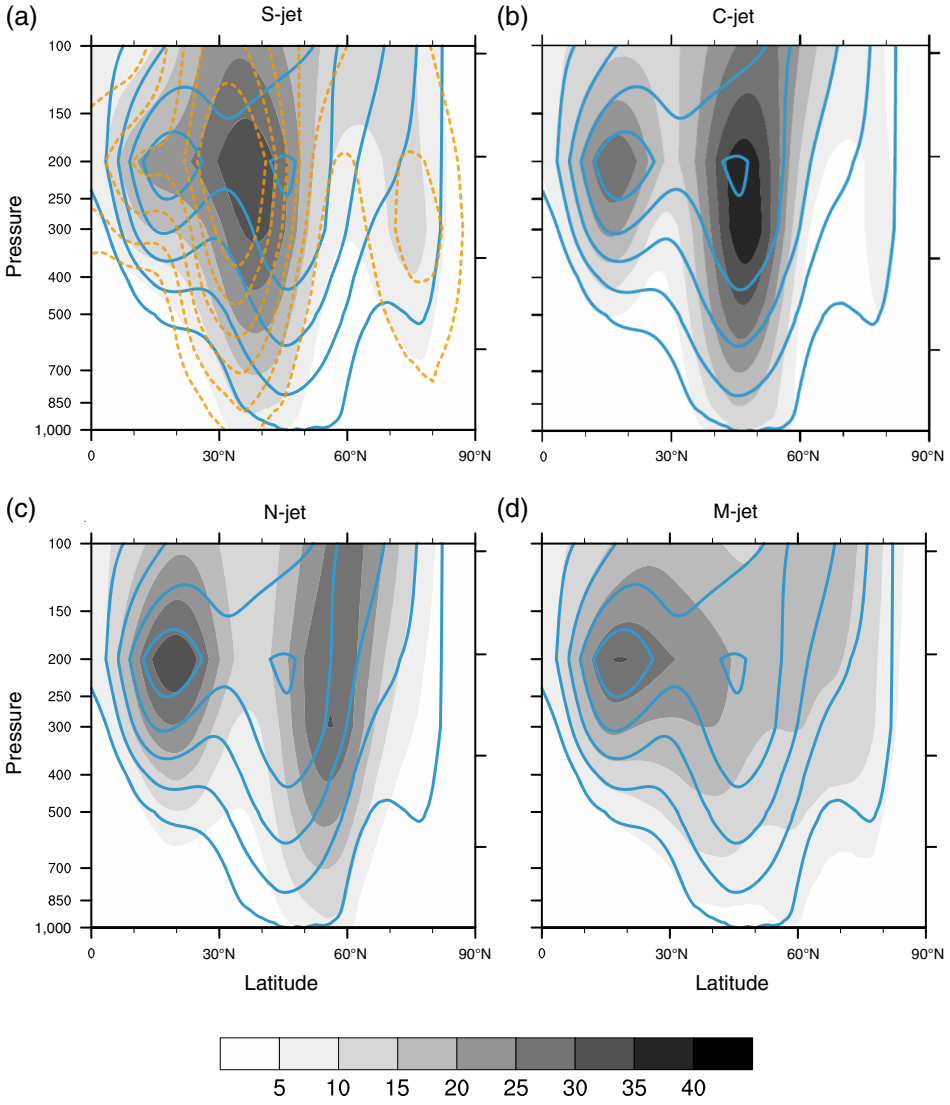

FIGURE 1 Wintertime (DJF) zonal wind (u) averaged over the North Atlantic sector [60°W–0°] as a function of latitude and pressure. Shown are the climatology (blue contours from 5 m s^{-1} in 5 m s^{-1} intervals) and u composites (gray shading in m s^{-1}) for the (a) southern jet (S-jet), (b) central jet (C-jet), (c) northern jet (N-jet) and (d) mixed jet (M-jet) configurations. Dashed orange contours in (a) represent the zonal-mean u profile for the 2009/2010 winter (from 5 m s^{-1} in 5 m s^{-1} intervals)

2010; Wettstein and Wallace, 2010). Because the North Atlantic jet is primarily eddy-driven, much of its wintertime variability is accounted for by a meridional shifting (Eichelberger and Hartmann, 2007; Athanasiadis *et al.*, 2010), also referred to as the North Atlantic Oscillation (NAO), that affects both the jet position and structure (Woollings *et al.*, 2010a; Madonna *et al.*, 2017). In its southernmost (i.e., negative NAO) position, the jet tends to be rather zonal, with little southwest-northeast tilt (Woollings *et al.*, 2010b). These synoptic-scale jet shifts have an intrinsic time scale of about 1–2 weeks (Feldstein, 2000; Hannachi *et al.*, 2012) and arise from eddy-mean flow interactions (Lorenz and Hartmann, 2003; Rivière and Orlanski, 2007).

Jet variability may also arise from changes in the balance of driving mechanisms. If the North Atlantic jet were to transition from being primarily eddy-driven to more equally eddy and thermally driven, for example, one would expect it to shift southward (Harnik *et al.*, 2014; Lachmy and Harnik, 2016). Such a transition seems to have occurred during the winter of 2009/2010 (subsequently referred to as the 2010 winter), when the jet was unusually southern, zonally-oriented and connected with the African jet downstream. It also bore the hallmarks of a merged jet (Harnik *et al.*, 2014)—notably, a single upper-tropospheric wind maximum located only slightly equatorward of the surface wind maximum (Figure 1a, orange dashed contours).

This raises the question of whether southward shifts of the North Atlantic jet stream can arise from different dynamics. On synoptic time scale, the southern configuration is part of the natural "shifting" variability of an eddy-driven jet (Eichelberger and Hartmann, 2007), which can show some amount of persistence (Lorenz and Hartmann, 2003; Barnes and Hartmann, 2010). But on seasonal or longer time scales (i.e., "climate") the southern configuration seems to reflect a more fundamental change from a jet that is predominantly eddy-driven to one that has a "merged" eddy-driven/subtropical character. Indeed, Harnik *et al.* (2014) found

evidence of enhanced thermal driving due to anomalous convection in the tropical Pacific during extended "southern jet" periods, suggesting an upstream source of zonal momentum for the 2010 winter Atlantic jet. To our knowledge, it is unresolved in the literature if and how southward shifts of the North Atlantic jet at different time scales are related.

This study combines the synoptic and climate viewpoints to clarify the dynamical nature of jet variability across times scales. We examine periods in the 35-year reanalysis record when the North Atlantic jet stream is shifted southwards and assumes a zonal orientation. We show that, even in the primarily eddy-driven North Atlantic sector, an interplay of eddy driving and thermal driving can create a merged jet on synoptic time scales as well as on seasonal time scales. We further show that the strong seasonal anomaly of winter 2010 was associated with an unusual number and persistence of synoptic southward jets shifts.

2 | DATA AND METHODS

Daily-mean temperature (T), zonal wind (u), and meridional wind (v) are computed from 6-hourly, 0.5-degree resolution ERA-Interim Reanalysis data on pressure levels (Dee *et al*., 2011) for all winter seasons (December to February, DJF) from 1979 to 2014. We apply a 10-day lowpass filter and a six-day highpass filter to isolate the low-frequency (background, denoted by *) and high-frequency (transient eddy, denoted by ′) components, respectively, of each field.

2.1 | Vertical jet shear

Jets are identified as regions where the pressure-weighted wind speed $U = (u^2 + v^2)^{1/2}$ between 100 and 400 hPa exceeds 30 m s^{-1}. We characterize the vertical shear (S) in the identified jets following Koch *et al*. (2006):

$$S_{200-500} = \frac{U_{200hPa} - U_{500hPa}}{U_{200hPa}} \tag{1}$$

Jets are considered "shallow" (confined to the upper troposphere) if $S_{200–500} > 0.4$ and "deep" (generally more barotropic) if $S_{200–500} < 0.4$.

2.2 | Transient eddies and eddy feedbacks

Eddy activity is measured by both 850-hPa (lower troposphere) heat fluxes ($v'T'_{850}$) and 300-hPa (upper troposphere) eddy kinetic energy ($EKE_{300} = \frac{u'^2 + v'^2}{2}$), metrics that capture well the signatures associated with the development and mature stage of transient eddies (Chang *et al*., 2002).

The nonlinear breaking of Rossby waves can influence jet position and strength via momentum fluxes (Simmons and Hoskins, 1978; Hoskins *et al*., 1983; Thorncroft *et al*., 1993; Lorenz and Hartmann, 2001). We distinguish between anticyclonic (LC1, NE–SW orientation) and cyclonic (LC2, NW–SE orientation) wave breaking, detected via filaments of potential vorticity (PV-streamers) according to the method of Martius *et al*. (2007). LC1 (LC2) occurs mostly on the equatorward (poleward) flank of the jet and pushes the jet polewards (equatorwards) (Thorncroft *et al*., 1993).

Eddy-mean flow interactions are diagnosed using the barotropic generation rate G (Mak and Cai, 1989; Rivière, 2008). It is defined as the scalar product between the horizontal component of the E-vector (**E**) and the deformation of the background flow (**D**):

$$G = \mathbf{E}\cdot\mathbf{D} \tag{2}$$

The E-vector indicates the propagation direction of transient eddies

$$\mathbf{E} = \begin{pmatrix} \frac{1}{2}\left(v'^2 - u'^2\right) \\ -u'v' \end{pmatrix} \tag{3}$$

and the deformation **D** describes the local rate of change in the shape of a fluid element due to stretching or shearing by the background flow

$$\mathbf{D} = \begin{pmatrix} \frac{\partial u^*}{\partial x} - \frac{\partial v^*}{\partial y} \\ \frac{\partial v^*}{\partial x} + \frac{\partial u^*}{\partial y} \end{pmatrix} \tag{4}$$

where x and y refer to the zonal and meridional direction, respectively. When G is negative (positive), the eddies lose energy to (extract energy from) the mean flow, thereby accelerating (decelerating) it.

2.3 | Thermal driving

As an indicator of tropical convection, we calculate anomalies in vertically integrated diabatic heating (i.e., "thermal driving"; iT) at each gridpoint following Li and Wettstein (2012) (see also Boer, 1986; Trenberth and Solomon, 1994).

$$iT = [R_T - R_S + H_S + LP] \tag{5}$$

where R_T is net downward radiation at the top of the atmosphere, R_S is the net downward radiation and H_S the upward sensible heat fluxes, both at the surface, L the latent heat of evaporation and P the precipitation rate. (This is a corrected version of Equation 1 in Li and Wettstein (2012), where an extra latent heating term H_L was erroneously included.)

Daily *iT* anomalies are calculated by removing the climatological daily mean. Regions with high values of *iT* are associated with anomalously strong upward velocities and anomalously negative outgoing longwave radiation (Li and Wettstein, 2012; Harnik *et al*., 2014), consistent with stronger deep convection.

2.4 | Jet configurations

We use four North Atlantic jet configurations identified via *k*-means clustering (Madonna *et al*., 2017). Briefly, empirical orthogonal functions are calculated from area-weighted daily anomalies of the lowpass-filtered zonal wind component (u^*) averaged in the lower troposphere between 900 and 700 hPa in the North Atlantic sector [$60^\circ W - 0^\circ W$, $15^\circ - 75^\circ N$]. We perform a *k*-means cluster analysis using the first five principal components (which explain 80% of the North Atlantic wintertime variance) and assign each day to a cluster. The southern (S), central (C), northern (N) and mixed (M) jet configurations shown in Figure 1 correspond to the canonical North Atlantic-European weather regimes (Vautard, 1990; Cassou, 2008; Madonna *et al*., 2017). Three of these configurations (S, C, N) are related to the jet positions identified by the zonal mean approach of Woollings *et al*. (2010a), though the distinction is not as clear when complex M-jet structures are forced into the zonal-mean classification (Madonna *et al*., 2017).

3 | RESULTS

A southward-shifted North Atlantic jet exhibits characteristics of a "merged jet" on synoptic time scales, just as suggested for longer (e.g., seasonal) time scales. The latitude-pressure composite of S-jet days shows a single jet located at approximately $36^\circ N$ (Figure 1a, shading). In contrast, composites of C- and N-jet days (Figure 1b, c, shading) show two distinct jets as in the climatology (blue contours), with the North Atlantic jet positioned poleward of 45°N and cleanly separated from the African subtropical jet at approximately 18°N. The M-jet composite (Figure 1d) gives the impression of a relatively broad, weak jet, but this is in fact an artifact of zonally averaging over a complex jet structure. The S-jet composite resembles the 2010 winter-mean jet (Figure 1a, orange contours), which was also anomalously zonal and southward-shifted (e.g., Harnik *et al*., 2014; Rivière and Drouard, 2015).

A range of diagnostics show that the S-jet is indeed less eddy-driven compared to other configurations, as expected for a merged eddy-thermally driven jet. During S-jet days, the jet is less barotropic (low percentage of deep jets in Figure 2e compared with other clusters in Figure 3, third row). Eddy heat fluxes ($v'T'_{850}$) are weak and localized over the Gulf stream region (compare Figure 2a with Figure 3, first row), while EKE_{300} is confined to the poleward flank of the jet (compare Figure 2c with Figure 3, second row). Poleward of the jet, cyclonic Rossby wave-breaking (LC2) dominates, maintaining the jet in its southern position (Thorncroft *et al*., 1993; Orlanski, 2003; Rivière and Orlanski, 2007); equatorward of the jet, anticyclonic wave-breaking (LC1) is limited to the jet exit region (Figure 2g, also in Franzke *et al*. (2011)). In comparison, the other jet configurations show frequent LC1 wave-breaking (Figure 3, fourth row), consistent with eddy-driven northward jet excursions. Finally, eddy-mean flow interaction is relatively weak for S-jet days, as assessed by the barotropic generation rate *G*. Negative values of *G* (Figure 4, shading) indicate regions of diverging E-vectors (red arrows) where eddies accelerate the mean flow. The S-jet configuration exhibits less negative (weaker) *G* compared to C-jet and M-jet composites. The values are comparable for the N-jet composite, but the N-jet eddies accelerate the mean flow over a larger region extending over northern and central Europe, where the E-vectors veer equatorward. Regression analyses yield a consistent message, confirming that differences in eddy activity between jet configurations are clear despite substantial variability within jet configurations (results for eddy heat flux shown in Figure S1, with regression amplitudes reaching approximately 20% of the composite spread for S-jet). Together, these diagnostics show reduced eddy activity and weaker eddy interaction with the background flow during S-jet periods.

The S-jet configuration also exhibits evidence of increased thermal driving on synoptic time scales. To assess this, we consider the potential for remote influences on the North Atlantic jet from convection anomalies over the tropical Pacific, due in part to sea surface temperature (SST) perturbations (Harnik *et al*., 2014), as measured by the thermal driving index *iT*. Positive *iT* anomalies over the tropical Pacific [150°E–120°W] indicate enhanced convection and are associated with the S-jet configuration (Figure 5a and S2, top left panel). The tropical Pacific *iT* anomalies are stronger for the most persistent S-jet events (Figure 5b), and quite stable overall, but slightly weaker at leads of 30 days (Figure S3). This enhanced convection upstream in the tropical Pacific has been proposed to act as a source of momentum for the North Atlantic jet downstream (Harnik *et al*., 2014; Martius, 2014). Note that *iT* signals in the tropical Atlantic are quite weak (Figure 5), suggesting that changes in "local" thermal driving are not instrumental for the S-jet configuration (Li and Wettstein, 2012), although they do seem to affect the zonal extent of the African jet (e.g., weaker Atlantic *iT* is associated with a retracted African jet in Figure 4a, black contours; see also Li and Wettstein (2012), their Figure 2). *iT* anomalies associated with the other jet configurations are much weaker

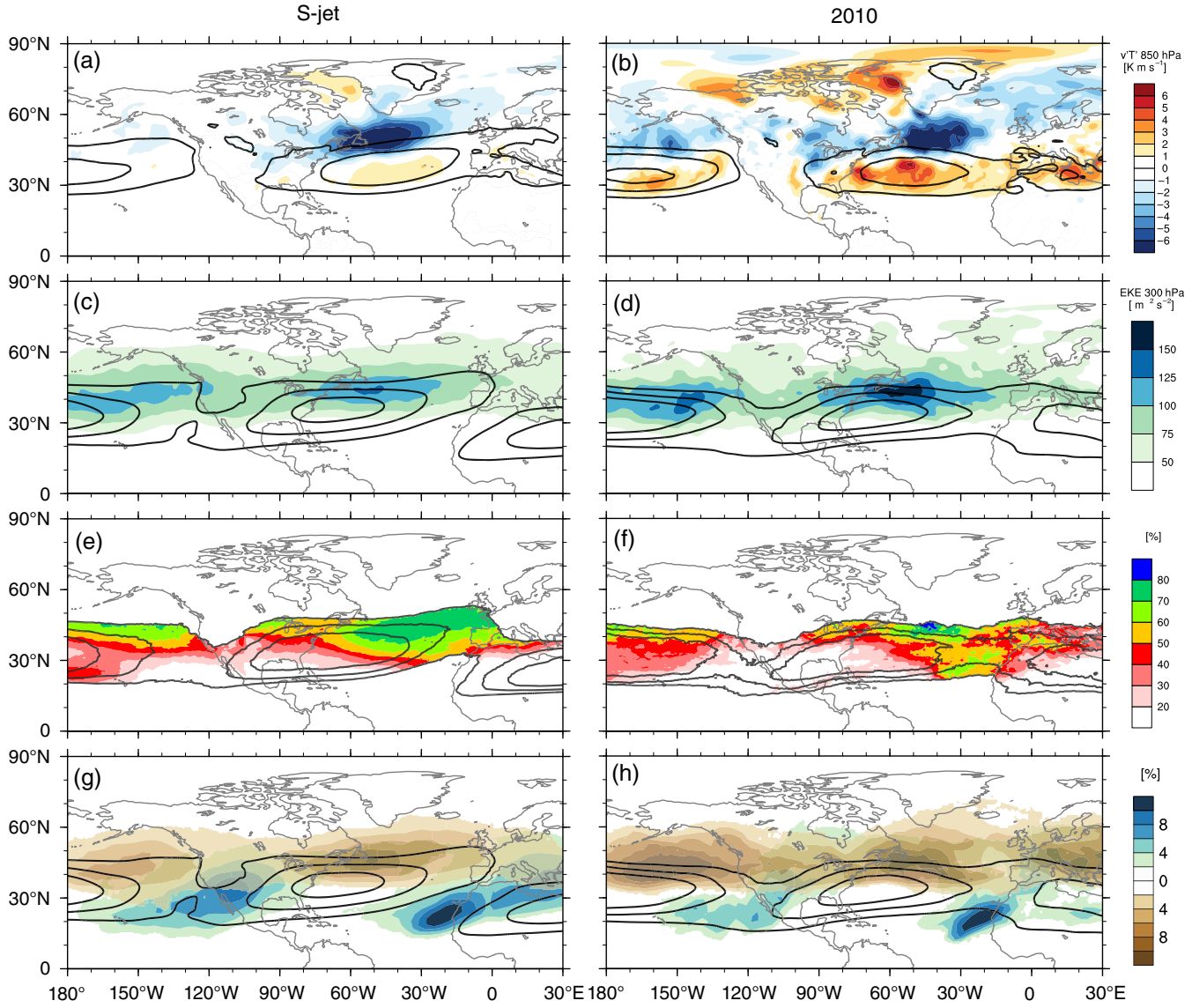

FIGURE 2 Comparison between the synoptic S-jet configuration (left) and the 2010 winter (right). (a, b) Eddy heat flux anomalies ($v'T'_{850}$, shading) and zonal wind at 850 hPa (contours). (c, d) Eddy kinetic energy (EKE_{300}, shading) and zonal wind at 300 hPa (contours). (e, f) Percentage of deep jets ($S < 0.4$, shading in %), and percentage of time that a jet is identified (i.e., wind speed averaged between 100 and 400 hPa >30 m s^{-1}, black contours at 40, 60, and 80%). (g, h) Rossby wave breaking (cyclonic/LC2 in brown, anticyclonic/LC1 in blue, in % of time) and zonal wind at 300 hPa (contours). Zonal wind contours are at 5, 10, and 15 m s^{-1} for 850 hPa (a, b) and at 20, 30, and 40 m s^{-1} for 300 hPa (c, d and g, h)

(Figure S3), suggesting a smaller role for thermal driving in their maintenance.

Repeating the analyses performed on the synoptic S-jet for the 2010 winter, we find a consistent picture of a merged jet that is more thermally driven and less eddy-driven. This allows us to link previous studies that suggested key roles for tropical heating (Harnik *et al*., 2014) and cyclonic wave breaking (Rivière and Drouard, 2015) for this particular winter season. Enhanced thermal driving from the tropical Pacific during the 2010 winter is similar to, though stronger than, the anomalies in the S-jet composite (Figure 5c,a). The *iT* signal in the S-jet composite is robust to removal of the 2010 winter (Figure S4). In addition, the 2010 winter is characterized by fewer deep, barotropic jet occurrences and less eddy activity, with EKE_{300} and $v'T'_{850}$ patterns comparable to the S-jet configuration (Figure 2, right vs. left column). We observe a high frequency of cyclonic wave breaking (LC2, Figure 2h), which produces weaker eddy momentum fluxes than LC1 (Rivière, 2011), but nonetheless acts to maintain the jet in a southern position (Barnes and Hartmann, 2010). The results collectively suggest that a change in the balance of driving mechanisms can occur across a range of time scales, producing a merged North Atlantic jet that lasts anywhere from several days to an entire season. The suppression of eddy feedbacks when the jet is particularly strong (Afargan and Kaspi, 2017) or southward-

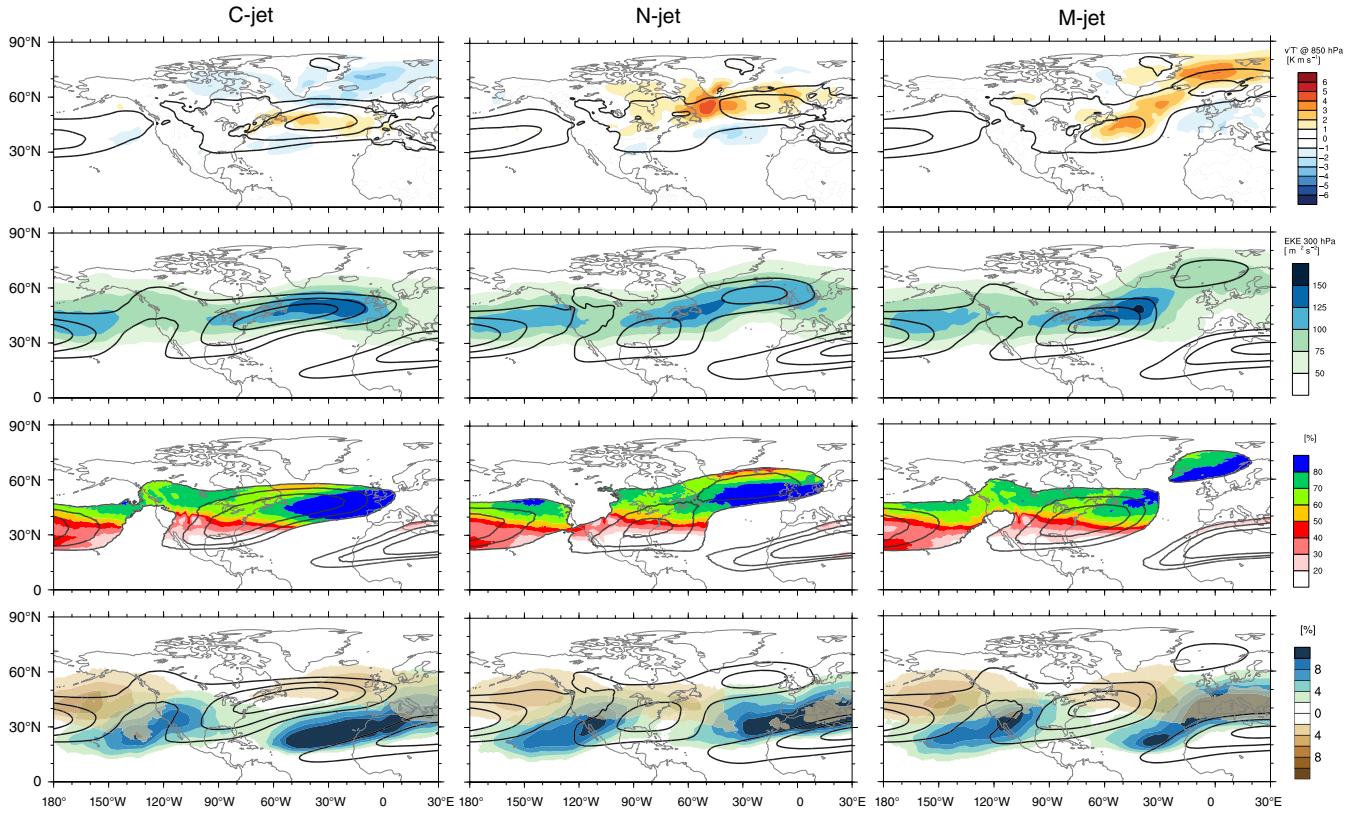

FIGURE 3 As in Figure 2, but for C-jet (first column), N-jet (second column) and M-jet (third column)

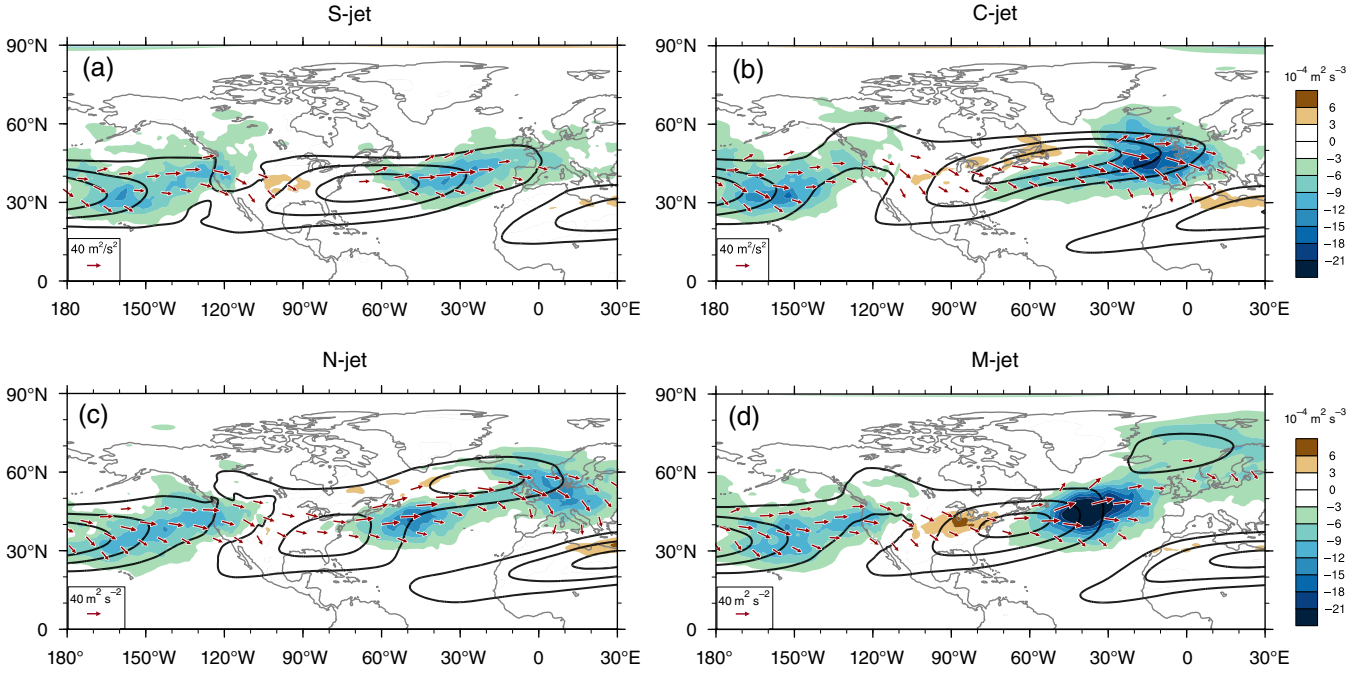

FIGURE 4 Composites of barotropic generation rate (G, shading in 10^{-4} m^2 s^{-3}), zonal wind at 300 hPa (u, contours at 20, 30, and 40 m s^{-1}) and E-vector at 300 hPa (red arrows, >30 m^2 s^{-2}, in m^2 s^{-2}) for the (a) southern jet (S-jet), (b) central jet (C-jet), (c) northern jet (N-jet) and (d) mixed jet (M-jet) configurations

shifted (Yuval *et al.*, 2018) results in a wind field that resembles the North Pacific both in its mean state and variability (see Section 4).

The unusual winter-mean jet of 2010 can in fact be understood as the result of an extremely high frequency of synoptic S-jet days. There are on average 20 S-jet days in a

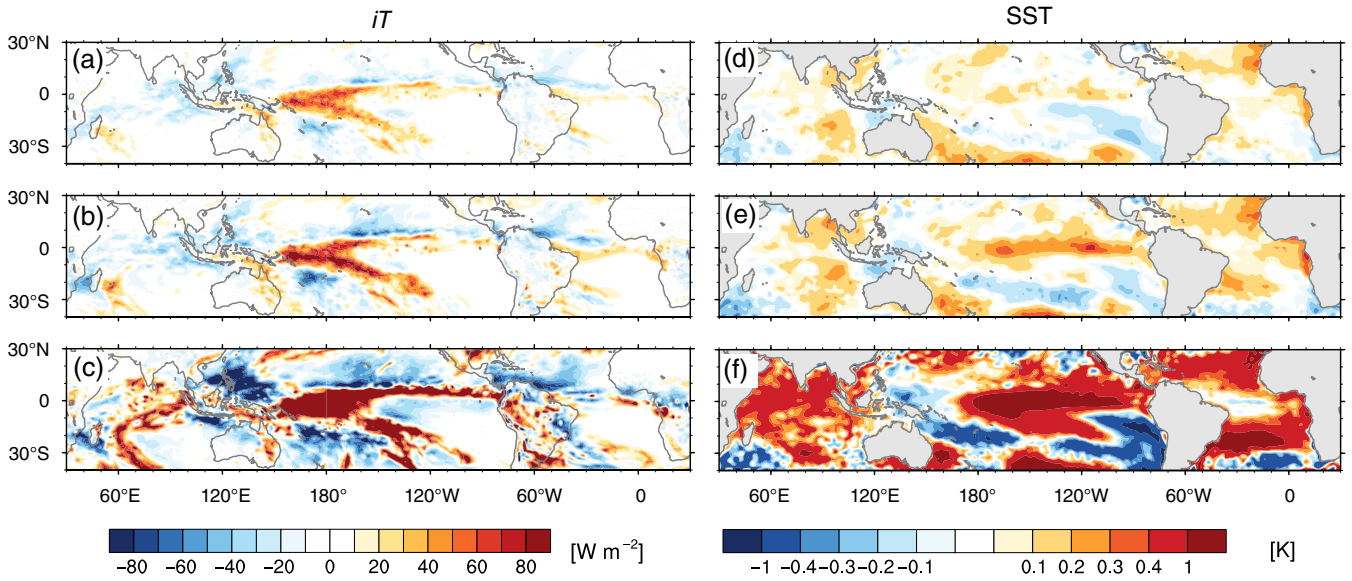

FIGURE 5 Left: composites of thermal driving index anomalies (*iT*, shading in W m^{-2}) at a 20-day lead for (a) all S-jet days, (b) persistent (lasting more than 10 days) S-jet periods and (c) S-jet days in the 2010 winter. Right: composites of SST anomalies (shading, in K) for (d) all S-jet days, (e) persistent S-jet periods and (f) S-jet days in the 2010 winter

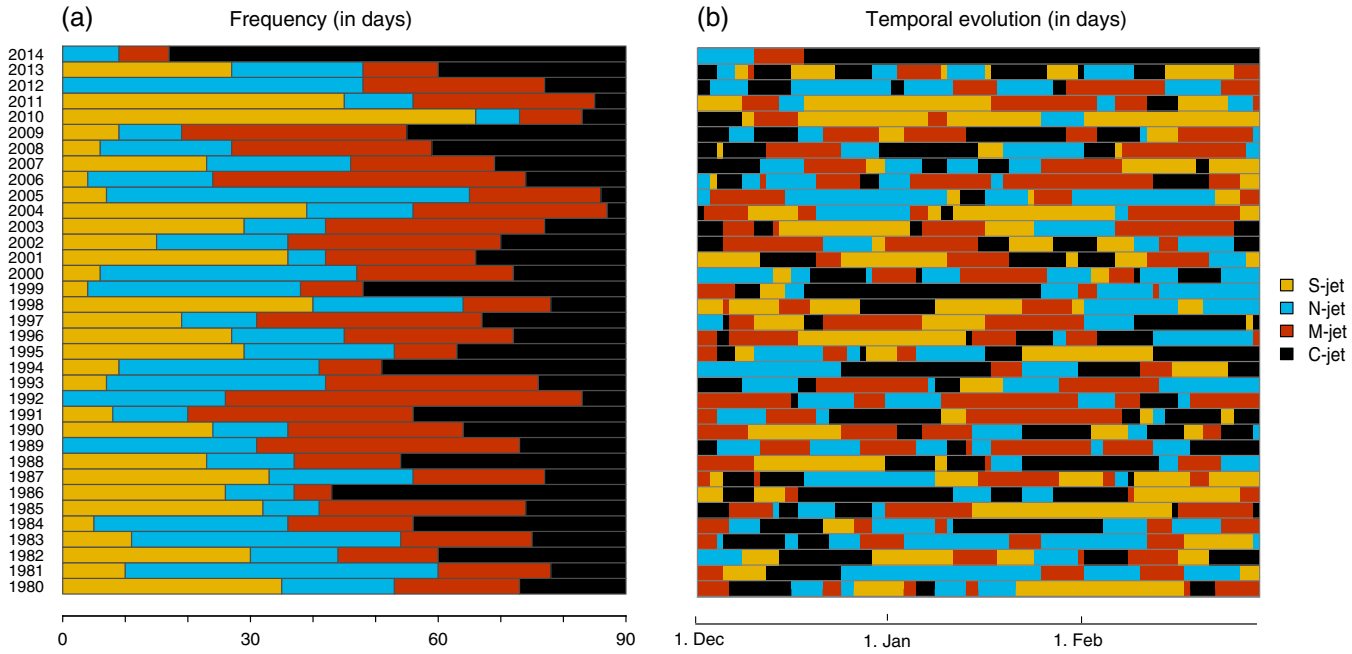

FIGURE 6 (a) Frequency (in days) of jet configurations for each DJF winter (1980–2014). (b) Temporal evolution of jet configurations for each DJF winter. The *x*-axis starts on 1 December and ends on 28 February (90 days). Year labels correspond to the January and February, such that 1980 is the winter season from December 1979 to February 1980

given winter, with large interannual variability (standard deviation of approximately 16 days) including some winter seasons (1989, 1992, 2012, and 2014) during which there are no S-jet occurrences (Figure 6a, orange bars). For the 2010 winter, there were 66 S-jet days concentrated in three prolonged events (Figure 6). The North Atlantic jet was in the S-configuration for over 70% of the season, making it the most extreme case of all 35 winters in the 1980–2014 record. The 2010 winter can thus be considered special insofar as it exhibits little intraseasonal variability and is dominated by the southern jet configuration.

Finally, the fact that S-jet alone of the four North Atlantic jet configurations shows evidence of a more subtropical, less eddy-driven nature suggests that it is somewhat special. This

may be why it occurs slightly less frequently overall, and why it is the only jet configuration that is completely absent during some winters (Figure 6).

4 | DISCUSSION

The influence of the tropical Pacific on the North Atlantic during S-jet periods is consistent with previous studies on tropical forcing of the extratropical atmospheric circulation. On daily time scales, tropical convection triggered by the Madden–Julian Oscillation (MJO) produces Rossby wave trains that can affect the North Atlantic (e.g., Matthews *et al*., 2004; Cassou, 2008; Lin *et al*., 2009). In particular, MJO phase 6 and 7 (convection in the central tropical Pacific) has been identified as a precursor of negative NAO conditions, and is associated with outgoing longwave radiation anomalies (cf. Figure 2 in Cassou, 2008) that resemble the *iT* anomaly pattern found 10–20 days prior to S-jet (Figure 5 and S3). On longer time scales, the North Atlantic may be affected by tropical SST anomalies such as those accompanying the El-Niño Southern Oscillation (ENSO). During El Niño events, when the eastern and central tropical Pacific are warmer than usual, there is a tendency for negative NAO conditions (Brönnimann, 2007; Li and Lau, 2012), although the relationship is quite noisy (Deser *et al*., 2017) as well as being both nonlinear and nonstationary (Greatbatch *et al*., 2004). The signal can propagate via different pathways, including the stratosphere (e.g., Bell *et al*., 2009; Ineson and Scaife, 2009; Butler and Polvani, 2011), the North Pacific (e.g., Li and Lau, 2012) or the tropical Atlantic (e.g., Sung *et al*., 2013) through suppression of local convection due to changes in the Walker circulation (e.g., Wang, 2002; Schwendike *et al*., 2014; Mbengue *et al*., 2019). The SST and *iT* anomalies in the tropical Pacific and tropical Atlantic are similar for the 2010 El-Niño and the S-jet composite, particularly when considering only persistent (>10 days) S-jet events (Figure 5). Despite the SST signals being weaker for S-jet compared to El Niño, it is possible that they have similar effects on the location of tropical convection, length of MJO cycles (Pohl and Matthews, 2007), and MJO teleconnections to the North Atlantic (Moon *et al*., 2011).

Other well-studied influences on the North Atlantic likely contributed to the unusually southern jet during the 2010 winter. In addition to the El Niño, the quasi-biennial oscillation was in its easterly phase, which is favorable for sudden stratospheric warmings (Richter *et al*., 2011; Fereday *et al*., 2012) that weaken the polar vortex (Holton and Tan, 1980). Indeed, a sudden stratospheric warming occurred in late January/early February 2010 (Dörnbrack *et al*., 2012; Butler *et al*., 2017). A weak vortex favors negative NAO conditions, both through stratosphere-troposphere coupling (Baldwin and Dunkerton, 1999, 2001) and by enhancing the tropospheric ENSO teleconnection to the North Atlantic (Jiménez-Esteve and Domeisen, 2018). A weak vortex is also associated with increased frequency of Greenland blocking (Papritz and Grams, 2018), which corresponds to the southern jet (Woollings *et al*., 2010a; Madonna *et al*., 2017). Furthermore, the 2010 winter featured a weak ridge over the eastern North Pacific (Figure 2d, also visible in S-jet composites Figure 2c), which has been shown to lead to increased cyclonic wave breaking and a southward-shifted jet in the North Atlantic (Rivière and Drouard, 2015). Finally, Eurasian snow cover interacting with the stratosphere can affect the North Atlantic circulation (Cohen *et al*., 2010). Relaxation experiments with the model from the European Centre for Medium-Range Weather Forecasts (ECMWF) indicate that no single factor mentioned above can account for the anomalous winter of 2010 (Jung *et al*., 2011), but a combination of factors together with internal atmospheric dynamical processes may offer an explanation (Jung *et al*., 2011; Santos *et al*., 2013; Hansen *et al*., 2017).

We have focused on the fact that the eddies are weaker during S-jet, but the eddy activity itself is also shifted equatorward (e.g., heat flux anomalies in Figures 2 and 3). This highlights a well-known chicken-or-egg dilemma: do changes in the jet alter the eddies, or is it the other way around? A hint could come from a phenomenon in the North Pacific known as the "mid-winter suppression" (Nakamura, 1992); at the peak of the cold season, when the jet and baroclinicity are strongest, the eddy kinetic energy undergoes a slight dip in strength. It is still debated what causes the midwinter suppression but factors suggested to be important include upstream seeding of the storm track (e.g., Nakamura, 1992; Park *et al*., 2010; Penny *et al*., 2010, 2013), diabatic processes (e.g., Chang, 2001), as well as the position and strength of the jet itself (e.g., Nakamura *et al*., 2002; Harnik and Chang, 2004; Deng and Mak, 2005; Afargan and Kaspi, 2017). Recent studies suggest that key for the suppression of eddy activity is a jet that is subtropical in nature, equatorward-shifted, and relatively strong (Woollings *et al*., 2018; Yuval *et al*., 2018; Yuval and Kaspi, 2018), which in general holds for S-jet.

In terms of North Atlantic jet variability, the 2013/2014 winter also stands out as exceptional (e.g., Davies, 2015; Rivière and Drouard, 2015; Watson *et al*., 2016). This winter exhibits the most sustained central jet (C-jet) in our record, persisting for 72 consecutive days (Figure 6, black bars), with a seasonal mean comparable to the C-jet composite (Figure 1b). A strong North Pacific ridge is visible in the C-jet composite as a poleward deflection of the North Pacific jet exit, and we observe equatorward E-vectors and enhanced anticyclonic wave breaking at the end of the North Atlantic jet (Figures 3 and 4b), consistent with Rivière and

Drouard (2015). Both the 2009/2010 and 2013/2014 winters were thus unusual from the climate perspective in that they are associated with strong seasonal anomalies (e.g., temperature and precipitation). From the synoptic perspective, however, the unusual signal arises from a high frequency of "regular" synoptic S-jet and C-jet configurations.

5 | CONCLUSIONS

The North Atlantic wintertime jet is primarily eddy-driven, but takes on a merged eddy-thermally driven character when it is located south of its climatological position. While this has been discussed for the 2010 winter (Harnik *et al*., 2014), the analyses here show altered dynamical behavior during southern jet excursions, regardless of time scale. On synoptic time scales, southern jet periods exhibit reduced eddy activity and weak eddy-mean flow interactions compared to other jet configurations. At the same time, they are associated with enhanced diabatic heating in the tropical Pacific that is maximized at leads of 10–20 days. The unusual winter mean of 2010 is found to reflect a high concentration of prolonged S-jet events making up 70% of the season (66 days compared to the typical 20 days).

This study represents a step towards bridging the weather and climate perspectives to better understand jet variability. It also offers alternative views on jet biases in climate models, such as whether the common problem of an overly steady, zonal North Atlantic jet (Anstey *et al*., 2013; Hannachi *et al*., 2013) results from too much time spent in the central jet configuration due to a misrepresentation of eddy-mean flow interactions or tropical-extratropical teleconnections.

ACKNOWLEDGEMENTS

The authors would like to thank Olivia Martius for providing the wave breaking classification and Michael Sprenger and Heini Wernli for the vertical jet shear classification. We thank David Battisti and Clio Michel for stimulating discussions and two anonymous reviewers for their constructive comments. The authors acknowledge funding from the Research Council of Norway (jetSTREAM grant 231716 and DynAMiTe grant 255027). ERA-Interim data have been obtained from the ECMWF public datasets: https://apps.ecmwf.int/datasets/.

ORCID

Erica Madonna https://orcid.org/0000-0002-8656-8187

REFERENCES

Afargan, H. and Kaspi, Y. (2017) A midwinter minimum in North Atlantic storm track intensity in years of a strong jet. *Geophysical Research Letters*, 44, 12511–12518.

Anstey, J.A., Davini, P., Gray, L.J., Woollings, T.J., Butchart, N., Cagnazzo, C., Christiansen, B., Hardiman, S.C., Osprey, S.M. and Yang, S. (2013) Multi-model analysis of Northern Hemisphere winter blocking: model biases and the role of resolution. *Journal of Geophysical Research: Atmospheres*, 118, 3956–3971.

Athanasiadis, P.J., Wallace, J.M. and Wettstein, J.J. (2010) Patterns of wintertime jet stream variability and their relation to the storm tracks. *Journal of the Atmospheric Sciences*, 67, 1361–1381.

Baldwin, M.P. and Dunkerton, T.J. (1999) Propagation of the Arctic Oscillation from the stratosphere to the troposphere. *Journal of Geophysical Research, Atmospheres*, 104, 30937–30946.

Baldwin, M.P. and Dunkerton, T.J. (2001) Stratospheric harbingers of anomalous weather regimes. *Science*, 294, 581–584.

Barnes, E.A. and Hartmann, D.L. (2010) Dynamical feedbacks and the persistence of the NAO. *Journal of the Atmospheric Sciences*, 67, 851–865.

Bell, C.J., Gray, L.J., Charlton-Perez, A.J., Joshi, M.M. and Scaife, A. A. (2009) Stratospheric communication of El Niño teleconnections to European winter. *Journal of Climate*, 22, 4083–4096.

Boer, G. (1986) A comparison of mass and energy budgets from two FGGE datasets and a GCM. *Monthly Weather Review*, 114, 885–902.

Brönnimann, S. (2007) Impact of El Niño–Southern Oscillation on European climate. *Reviews of Geophysics*, 45, RG3003.

Butler, A.H. and Polvani, L.M. (2011) El Niño, La Niña, and stratospheric sudden warmings: a reevaluation in light of the observational record. *Geophysical Research Letters*, 38, L13807.

Butler, A.H., Sjoberg, J.P., Seidel, D.J. and Rosenlof, K.H. (2017) A sudden stratospheric warming compendium. *Earth System Science Data*, 9, 63–76.

Cassou, C. (2008) Intraseasonal interaction between the Madden–Julian oscillation and the North Atlantic Oscillation. *Nature*, 455, 523–527.

Chang, E.K. (2001) GCM and observational diagnoses of the seasonal and interannual variations of the Pacific storm track during the cool season. *Journal of the Atmospheric Sciences*, 58, 1784–1800.

Chang, E.K., Lee, S. and Swanson, K.L. (2002) Storm track dynamics. *Journal of Climate*, 15, 2163–2183.

Cohen, J., Foster, J., Barlow, M., Saito, K. and Jone, J. (2010) Winter 2009-2010: a case study of an extreme Arctic oscillation event. *Geophysical Research Letters*, 37, L17707.

Davies, H.C. (2015) Weather chains during the 2013/2014 winter and their significance for seasonal prediction. *Nature Geoscience*, 8, 833–837.

Dee, D.P., Uppala, S.M., Simmons, A.J., Berrisford, P., Poli, P., Kobayashi, S., Andrae, U., Balmaseda, M.A., Balsamo, G., Bauer, P., Bechtold, P., Beljaars, A.C.M., van de Berg, L., Bidlot, J., Bormann, N., Delsol, C., Dragani, R., Fuentes, M., Geer, A.J., Haimberger, L., Healy, S.B., Hersbach, H., Hólm, E.V., Isaksen, L., Kållberg, P., Köhler, M., Matricardi, M., McNally, A. P., Monge-Sanz, B.M., Morcrette, J.-J., Park, B.-K., Peubey, C., de Rosnay, P., Tavolato, C., Thépaut, J.-N. and Vitart, F. (2011) The ERA-Interim reanalysis: configuration and performance of the data

assimilation system. *Quarterly Journal of the Royal Meteorological Society*, 137, 553–597.

Deng, Y. and Mak, M. (2005) An idealized model study relevant to the dynamics of the midwinter minimum of the Pacific storm track. *Journal of the Atmospheric Sciences*, 62, 1209–1225.

Deser, C., Simpson, I.R., McKinnon, K.A. and Phillips, A.S. (2017) The Northern Hemisphere extratropical atmospheric circulation response to ENSO: how well do we know it and how do we evaluate models accordingly? *Journal of Climate*, 30, 5059–5082.

Dörnbrack, A., Pitts, M.C., Poole, L.R., Orsolini, Y., Nishii, K. and Nakamura, H. (2012) The 2009–2010 Arctic stratospheric winter-general evolution, mountain waves and predictability of an operational weather forecast model. *Atmospheric Chemistry and Physics*, 12, 3659–3675.

Eichelberger, S.J. and Hartmann, D.L. (2007) Zonal jet structure and the leading mode of variability. *Journal of Climate*, 20, 5149–5163.

Feldstein, S.B. (2000) The timescale, power spectra, and climate noise properties of teleconnection patterns. *Journal of Climate*, 13, 4430–4440.

Fereday, D.R., Maidens, A., Arribas, A., Scaife, A.A. and Knight, J.R. (2012) Seasonal forecasts of northern hemisphere winter 2009/10. *Environmental Research Letters*, 7, 034031.

Franzke, C., Woollings, T. and Martius, O. (2011) Persistent circulation regimes and preferred regime transitions in the North Atlantic. *Journal of the Atmospheric Sciences*, 68, 2809–2825.

Greatbatch, R.J., Lu, J. and Peterson, K.A. (2004) Nonstationary impact of ENSO on Euro-Atlantic winter climate. *Geophysical Research Letters*, 31, L02208.

Hannachi, A., Woollings, T. and Fraedrich, K. (2012) The North Atlantic jet stream: a look at preferred positions, paths and transitions. *Quarterly Journal of the Royal Meteorological Society*, 138, 862–877.

Hannachi, A., Barnes, E.A. and Woollings, T. (2013) Behaviour of the winter North Atlantic eddy-driven jet stream in the CMIP3 integrations. *Climate Dynamics*, 41, 995–1007.

Hansen, F., Greatbatch, R.J., Gollan, G., Jung, T. and Weisheimer, A. (2017) Remote control of North Atlantic oscillation predictability via the stratosphere. *Quarterly Journal of the Royal Meteorological Society*, 143, 706–719.

Harnik, N. and Chang, E.K. (2004) The effects of variations in jet width on the growth of baroclinic waves: implications for midwinter Pacific storm track variability. *Journal of the Atmospheric Sciences*, 61, 23–40.

Harnik, N., Galanti, E., Martius, O. and Adam, O. (2014) The anomalous merging of the African and North Atlantic jet streams during the Northern Hemisphere winter of 2010. *Journal of Climate*, 27, 7319–7334.

Held, I.M. (1975) Momentum transport by quasi-geostrophic eddies. *Journal of the Atmospheric Sciences*, 32, 1494–1497.

Held, I.M. and Hou, A.Y. (1980) Nonlinear axially symmetric circulations in a nearly inviscid atmosphere. *Journal of the Atmospheric Sciences*, 37, 515–533.

Holton, J.R. and Tan, H.-C. (1980) The influence of the equatorial quasi-biennial oscillation on the global circulation at 50 mb. *Journal of the Atmospheric Sciences*, 37, 2200–2208.

Hoskins, B.J., James, I.N. and White, G.H. (1983) The shape, propagation and mean-flow interaction of large-scale weather systems. *Journal of the Atmospheric Sciences*, 40, 1595–1612.

Ineson, S. and Scaife, A. (2009) The role of the stratosphere in the European climate response to El Niño. *Nature Geoscience*, 2, 32–36.

Jiménez-Esteve, B. and Domeisen, D.I. (2018) The tropospheric pathway of the ENSO–North Atlantic teleconnection. *Journal of Climate*, 31, 4563–4584.

Jung, T., Vitart, F., Ferranti, L. and Morcrette, J.-J. (2011) Origin and predictability of the extreme negative NAO winter of 2009/10. *Geophysical Research Letters*, 38, L07701.

Koch, P., Wernli, H. and Davies, H.C. (2006) An event-based jet-stream climatology and typology. *International Journal of Climatology*, 26, 283–301.

Lachmy, O. and Harnik, N. (2016) Wave and jet maintenance in different flow regimes. *Journal of the Atmospheric Sciences*, 73, 2465–2484.

Lee, S. and Kim, H.-K. (2003) The dynamical relationship between subtropical and eddy-driven jets. *Journal of the Atmospheric Sciences*, 60, 1490–1503.

Li, Y. and Lau, N.-C. (2012) Contributions of downstream eddy development to the teleconnection between ENSO and the atmospheric circulation over the North Atlantic. *Journal of Climate*, 25, 4993–5010.

Li, C. and Wettstein, J.J. (2012) Thermally driven and eddy-driven jet variability in reanalysis. *Journal of Climate*, 25, 1587–1596.

Lin, H., Brunet, G. and Derome, J. (2009) An observed connection between the North Atlantic Oscillation and the Madden–Julian oscillation. *Journal of Climate*, 22, 364–380.

Lorenz, D.J. and Hartmann, D.L. (2001) Eddy-zonal flow feedback in the Southern Hemisphere. *Journal of the Atmospheric Sciences*, 58, 3312–3327.

Lorenz, D.J. and Hartmann, D.L. (2003) Eddy-zonal flow feedback in the Northern Hemisphere winter. *Journal of Climate*, 16, 1212–1227.

Madonna, E., Li, C., Grams, C.M. and Woollings, T. (2017) The link between eddy-driven jet variability and weather regimes in the North Atlantic-European sector. *Quarterly Journal of the Royal Meteorological Society*, 143, 2960–2972.

Mak, M. and Cai, M. (1989) Local barotropic instability. *Journal of the Atmospheric Sciences*, 46, 3289–3311.

Martius, O. (2014) A lagrangian analysis of the Northern Hemisphere subtropical jet. *Journal of the Atmospheric Sciences*, 71, 2354–2369.

Martius, O., Schwierz, C. and Davies, H.C. (2007) Breaking waves at the tropopause in the wintertime northern hemisphere: climatological analyses of the orientation and the theoretical LC1/2 classification. *Journal of the Atmospheric Sciences*, 64, 2576–2592.

Matthews, A.J., Hoskins, B.J. and Masutani, M. (2004) The global response to tropical heating in the Madden–Julian oscillation during the northern winter. *Quarterly Journal of the Royal Meteorological Society*, 130, 1991–2011.

Mbengue, C.O., Woollings, T., Dacre, H.F. and Hodges, K.I. (2019) The roles of static stability and tropical–extratropical interactions in the summer interannual variability of the North Atlantic sector. *Climate Dynamics*, 52, 1299–1315.

Moon, J.-Y., Wang, B. and Ha, K.-J. (2011) ENSO regulation of MJO teleconnection. *Climate Dynamics*, 37, 1133–1149.

Nakamura, H. (1992) Midwinter suppression of baroclinic wave activity in the Pacific. *Journal of the Atmospheric Sciences*, 49, 1629–1642.

Nakamura, H., Izumi, T. and Sampe, T. (2002) Interannual and decadal modulations recently observed in the Pacific storm track activity and east Asian winter monsoon. *Journal of Climate*, 15, 1855–1874.

Orlanski, I. (2003) Bifurcation in eddy life cycles: implications for storm track variability. *Journal of the Atmospheric Sciences*, 60, 993–1023.

Panetta, R.L. (1993) Zonal jets in wide baroclinically unstable regions: persistence and scale selection. *Journal of the Atmospheric Sciences*, 50, 2073–2106.

Papritz, L. and Grams, C.M. (2018) Linking low-frequency large-scale circulation patterns to cold air outbreak formation in the northeastern North Atlantic. *Geophysical Research Letters*, 45, 2542–2553.

Park, H.-S., Chiang, J.C. and Son, S.-W. (2010) The role of the central Asian mountains on the midwinter suppression of North Pacific storminess. *Journal of the Atmospheric Sciences*, 67, 3706–3720.

Penny, S., Roe, G.H. and Battisti, D.S. (2010) The source of the mid-winter suppression in storminess over the North Pacific. *Journal of Climate*, 23, 634–648.

Penny, S.M., Battisti, D.S. and Roe, G.H. (2013) Examining mechanisms of variability within the Pacific storm track: upstream seeding and jet-core strength. *Journal of Climate*, 26, 5242–5259.

Pohl, B. and Matthews, A.J. (2007) Observed changes in the lifetime and amplitude of the Madden–Julian oscillation associated with interannual ENSO sea surface temperature anomalies. *Journal of Climate*, 20, 2659–2674.

Rhines, P.B. (1975) Waves and turbulence on a β-plane. *Journal of Fluid Mechanics*, 69, 417–443.

Richter, J.H., Matthes, K., Calvo, N. and Gray, L.J. (2011) Influence of the quasi-biennial oscillation and El Niño–Southern Oscillation on the frequency of sudden stratospheric warmings. *Journal of Geophysical Research: Atmospheres*, 116, D20111.

Rivière, G. (2008) Barotropic regeneration of upper-level synoptic disturbances in different configurations of the zonal weather regime. *Journal of the Atmospheric Sciences*, 65, 3159–3178.

Rivière, G. (2011) A dynamical interpretation of the poleward shift of the jet streams in global warming scenarios. *Journal of the Atmospheric Sciences*, 68, 1253–1272.

Rivière, G. and Drouard, M. (2015) Understanding the contrasting North Atlantic Oscillation anomalies of the winters of 2010 and 2014. *Geophysical Research Letters*, 42, 6868–6875.

Rivière, G. and Orlanski, I. (2007) Characteristics of the Atlantic storm-track eddy activity and its relation with the North Atlantic Oscillation. *Journal of the Atmospheric Sciences*, 64, 241–266.

Santos, J.A., Woollings, T. and Pinto, J.G. (2013) Are the winters 2010 and 2012 archetypes exhibiting extreme opposite behavior of the North Atlantic jet stream? *Monthly Weather Review*, 141, 3626–3640.

Schneider, E.K. (1977) Axially symmetric steady-state models of the basic state for instability and climate studies. Part II. Nonlinear circulations. *Journal of the Atmospheric Sciences*, 34, 280–296.

Schwendike, J., Govekar, P., Reeder, M.J., Wardle, R., Berry, G.J. and Jakob, C. (2014) Local partitioning of the overturning circulation in the tropics and the connection to the Hadley and Walker circulations. *Journal of Geophysical Research: Atmospheres*, 119, 1322–1339.

Simmons, A.J. and Hoskins, B.J. (1978) The life cycle of some nonlinear baroclinic waves. *Journal of the Atmospheric Sciences*, 35, 414–432.

Son, S.-W. and Lee, S. (2005) The response of westerly jets to thermal driving in a primitive equation model. *Journal of the Atmospheric Sciences*, 62, 3741–3757.

Sung, M.-K., Ham, Y.-G., Kug, J.-S. and An, S.-I. (2013) An alterative effect by the tropical North Atlantic SST in intraseasonally varying El Niño teleconnection over the North Atlantic. *Tellus A: Dynamic Meteorology and Oceanography*, 65, 19863.

Thorncroft, C., Hoskins, B.J. and McIntyre, M.E. (1993) Two paradigms of baroclinic wave life cycle behaviour. *Quarterly Journal of the Royal Meteorological Society*, 119, 17–55.

Trenberth, K. and Solomon, A. (1994) The global heat balance: heat transports in the atmosphere and ocean. *Climate Dynamics*, 10, 107–134.

Vautard, R. (1990) Multiple weather regimes over the North Atlantic: analysis of precursors and successors. *Monthly Weather Review*, 118, 2056–2081.

Wang, C. (2002) Atlantic climate variability and its associated atmospheric circulation cells. *Journal of Climate*, 15, 1516–1536.

Watson, P.A., Weisheimer, A., Knight, J.R. and Palmer, T. (2016) The role of the tropical West Pacific in the extreme Northern Hemisphere winter of 2013/2014. *Journal of Geophysical Research: Atmospheres*, 121, 1698–1714.

Wettstein, J.J. and Wallace, J.M. (2010) Observed patterns of month-to-month storm-track variability and their relationship to the background flow. *Journal of the Atmospheric Sciences*, 67, 1420–1437.

Woollings, T., Hannachi, A. and Hoskins, B. (2010a) Variability of the North Atlantic eddy-driven jet stream. *Quarterly Journal of the Royal Meteorological Society*, 136, 856–868.

Woollings, T., Hannachi, A., Hoskins, B. and Turner, A. (2010b) A regime view of the North Atlantic Oscillation and its response to anthropogenic forcing. *Journal of Climate*, 23, 1291–1307.

Woollings, T., Barnes, E., Hoskins, B., Kwon, Y.-O., Lee, R.W., Li, C., Madonna, E., McGraw, M., Parker, T., Rodrigues, R., Spensberger, C. and Williams, K. (2018) Daily to decadal modulation of jet variability. *Journal of Climate*, 31, 1297–1314.

Yuval, J. and Kaspi, Y. (2018) Eddy sensitivity to jet characteristics. *Journal of the Atmospheric Sciences*, 75, 1371–1383.

Yuval, J., Afargan, H. and Kaspi, Y. (2018) The relation between the seasonal changes in jet characteristics and the Pacific Midwinter Minimum in eddy activity. *Geophysical Research Letters*, 45, 9995–10002.

SUPPORTING INFORMATION

Additional supporting information may be found online in the Supporting Information section at the end of this article.

How to cite this article: Madonna E, Li C, Wettstein JJ. Suppressed eddy driving during southward excursions of the North Atlantic jet on synoptic to seasonal time scales. *Atmos Sci Lett*. 2019;20:e937. https://doi.org/10.1002/asl.937